

Derivation and application of *ab initio* $\text{Nb}^{5+}-\text{O}^{2-}$ short-range effective pair potentials in shell-model simulations of KNbO_3 and KTaO_3

H. Donnerberg and M. Exner

Department of Physics, University of Osnabrück, D-49069 Osnabrück, Federal Republic of Germany

(Received 19 August 1993; revised manuscript received 4 November 1993)

We derive an *ab initio* $\text{Nb}^{5+}-\text{O}^{2-}$ short-range pair potential appropriate to KNbO_3 , which is based on suitable cluster Hartree-Fock calculations. The cluster to be chosen must necessarily represent a larger portion of KNbO_3 crystals than a lone $\text{Nb}^{5+}-\text{O}^{2-}$ pair embedded in the appropriate Madelung potential. Our final Hartree-Fock pair potential derived from (embedded) $(\text{NbO}_6)^{7-}$ cluster calculations is in good agreement with a corresponding empirical potential obtained from fitting procedures to macroscopic properties of KNb_3O_8 . Both potentials generate the cubic phase of KNbO_3 . Finally, the implications of these two $\text{Nb}^{5+}-\text{O}^{2-}$ pair potentials are discussed by means of shell-model defect simulations in KNbO_3 and KTaO_3 .

I. INTRODUCTION

Potential simulation methods are well known to play an important role in solid-state and material sciences. The Born-Oppenheimer approximation allows one to separate the electronic from nuclear degrees of freedom. Then by considering only the nuclear sub-Hamiltonian for various crystal geometries, the effective crystal potential is obtained as a function of nuclear coordinates. This potential, of course, absorbs in an averaged way all those electronic properties which influence the crystal bonding. Effective potentials are useful to investigate perfect lattice properties as well as defect processes in crystalline materials.

Simulation studies by means of such potentials are in particular very efficient in all cases where interionic/interatomic pair potentials constitute the dominant terms. This is true, for example, in ionic and semi-ionic materials. Many systems of technological interest, e.g., oxides, fall into this category. The success and scope of field is evident from recent investigations on complex oxide crystals such as BaTiO_3 ,¹ La_2CuO_4 ,² YIG ,³ and LiNbO_3 ,⁴ using a pair-potential shell model. For an overview on simulation methods in solid-state theory we refer the reader to Ref. 5.

The validity of any potential simulation study depends to considerable extent on the quality of the pair potentials used. Besides the traditional empirical approach, in which potentials are obtained by suitable fitting procedures to macroscopic crystal properties,⁵ there is an increasing interest in deriving pair potentials from *ab initio* calculations.

In this contribution we discuss the derivation of an *ab initio* $\text{Nb}^{5+}-\text{O}^{2-}$ pair potential appropriate to the perovskite-type KNbO_3 . This potential is intended to be used in shell-model simulations to elucidate the dominant defect structures in KNbO_3 as well as off-center displacements of Nb^{5+} impurities in KTaO_3 . A few results of these simulations are presented in the last section of this paper. A general discussion of the defect structure in

KNbO_3 and in KTaO_3 is deferred to a forthcoming paper.

II. DERIVATION OF POTENTIAL PARAMETERS

In order to facilitate the understanding of what follows we start by summarizing some basic facts concerning the shell model.^{5,6} Conceptually shell-model calculations are based on an ionic crystal model assuming formal (integral) ionic charges and dominating pairwise interionic potentials. There are given as long-range Coulomb interactions and short-range potentials resulting from the Pauli exclusion principle and interionic correlation effects. Short-range terms are conveniently described using Buckingham potentials:

$$V(r) = Ae^{-r/\rho} - C/r^6. \quad (2.1)$$

The van der Waals potential $-C/r^6$ occurring on the right side in (2.1) is designed to model the interionic correlations. The potential parameters A , ρ , and C depend on the interacting ion species and in most cases to some extent on the crystalline environment. We note that the use of integral ionic charges does not imply severe restrictions to purely ionic materials. This is true, because short-range potentials of the type introduced above are able (at least partly) to account for covalency and charge-transfer effects. The advantage of using integral ionic charges in potential simulation studies is based on the observation that electrostatic Madelung terms provide the dominant crystal energy contributions leading to reliable predictions of lattice- and defect-formation energies. A question of debate, however, could be given by the simplifying assumption of interionic pairwise potentials. Their use is justified so far by the success in modeling complex materials (see the Introduction).

The correct description of optical-phonon modes and the high-frequency dielectric constants forces one to introduce electronic polarizability of crystal ions. In the shell model each ion consists of a massive core (charge X , mass M) to which the shell of valence electrons (charge

Y , mass 0) is coupled via an isotropic harmonic restoring force (force constant k). The formal ionic charge is given by $Q = X + Y$ and the (free) electronic polarizability by

$$\alpha = Y^2/k. \quad (2.2)$$

It is useful to note that all short-range ion-ion potentials are defined as acting between different ion shells. As a consequence, the true electronic polarizability of the ions becomes crystal dependent, which is an important physical effect (especially for anions) that is simply and economically described by the shell model. Thus, it follows that in order to develop a reliable potential model for a given crystal the short-range potential parameters A, ρ, C for each ion-ion pair as well as the shell parameters Y, k belonging to each polarizable ion need to be specified.

In principle, two methods can be devised for deriving these parameters. In the empirical approach, mentioned in the Introduction, the unknown parameters are treated as variables to adjust calculated perfect crystal properties (crystal structure, elastic and dielectric constants) to the respective experimental data. Of course, successful application of this method presupposes sufficient experimental data to be known. Moreover, empirical potentials derived this way are strictly valid only at the observed perfect lattice spacings. This implies a strong need for theoretical methods, in particular for calculation of short-range potentials. Besides electron-gas procedures,^{5,7} based on the free-electron-gas local-density approximation energy functional and on the superposition of the ionic electronic charge densities, one may use *ab initio* cluster calculations. In particular for semi-ionic crystals *ab initio* methods should be preferred, because covalency effects are totally neglected with the electron-gas approach. Several examples for *ab initio* derived short-range potentials are known from literature.⁸⁻¹⁵

Thus, in the case of KNbO₃ we employed *ab initio* self-consistent field linear combination of atomic orbitals-molecular-orbitals (SCF-LCAO-MO) cluster calculations. Two types of clusters were considered in order to derive the short-range niobium-oxygen interaction, i.e., a simple Nb⁵⁺-O²⁻ pair and a more complex (NbO₆)⁷⁻ cluster. Both fragments were embedded in an appropriate set of point charges. Figure 1, for example, shows the (NbO₆)⁷⁻ cluster with its nearest potassium and niobium neighbors. The basis functions were chosen to be SV-21 (Huzinaga¹⁶) for Nb and the set of Dunning and Hay,¹⁷ modified by totally breaking up the p contractions and by augmenting with diffuse p - and polarizing d -type functions, for the oxygen ions. As a consequence of our improved basis set quality we expect possible basis set superposition errors¹⁸ to be substantially lower than those estimated for oxygen ions in MgO using a triple zeta valence (TZV) basis set (1.5 eV, Ref. 19).

One of our aims was to compare the *ab initio* potential with a given empirical Nb⁵⁺-O²⁻ potential. As the latter has been fixed to be a pure Born-Mayer exponential function,²⁰ it was reasonable to employ the Hartree-Fock approximation without correlation interaction in all of our cluster calculations and to fit the results with a Born-Mayer potential as well.

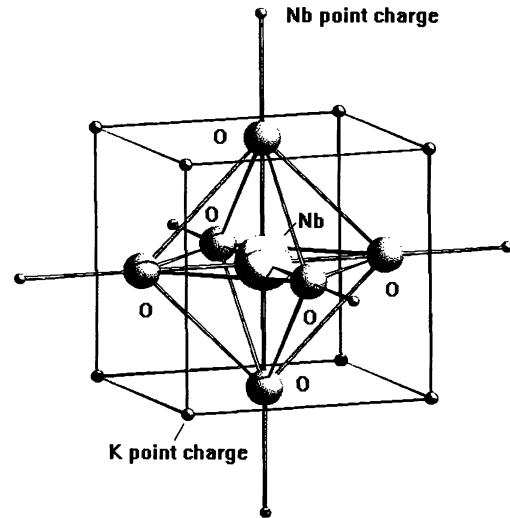


FIG. 1. (NbO₆)⁷⁻ quantum cluster with its nearest potassium and niobium (point charge) neighbors. Spheres do not correspond to known ion radii.

Short-range potential energies have been calculated for various cluster geometries according to the following formula:

$$V_{SR}^{Nb^{5+}-O^{2-}} = \frac{1}{n_{NbO}} \left[E_c^{HF} - \sum E_{self}^{HF} - E_{cb} - \sum V_{SR}^{O^{2-}-O^{2-}} - E_{pol} \right]. \quad (2.3)$$

n_{NbO} denotes the number of the Nb-O bonds in the cluster, E_c^{HF} the quantum mechanical cluster energy, $\sum E_{self}^{HF}$ is the sum of ionic self-energies, E_{cb} is the rigid-ion Coulomb contribution according to the formal charge model, $\sum V_{SR}^{O^{2-}-O^{2-}}$ is the occurring oxygen-oxygen short-range interactions and E_{pol} , finally, anionic polarization term. Ionic self-energies E_{self}^{HF} have been extracted by treating one ion at a time quantum mechanically and the other ions as point charges consistent with the respective cluster geometry. In order to be consistent with the empirical KNbO₃ potential model, $\sum V_{SR}^{O^{2-}-O^{2-}}$ in (2.3) has been taken over from that model. It is noted that Catlow and Hayns¹⁵ derived this anionic interaction as well from *ab initio* calculations. Since then it has been successfully applied to many simulation studies of oxides. Thus, we feel there is no need to replace this potential by another one. To avoid double counting effects when using *ab initio* short-range potentials in shell-model simulations, polarization terms must be either subtracted out from these potentials as was done in Eq. (2.3) or a procedure should be devised where electronic polarization of ions does not occur. E_{pol} in Eq. (2.3) consists of three different parts all of which are resulting from core-shell polarization, i.e., they arise from transcending from a rigid ion to a shell-model description:

$$E_{pol} = E_{pol}^{cb} + E_{pol}^{Harm} + E_{pol}^{SR}. \quad (2.4)$$

$E_{\text{pol}}^{\text{cb}}$ denoted corrections to E_{cb} defined above, $E_{\text{pol}}^{\text{Harm}}$ is the harmonic polarization energy, and $E_{\text{pol}}^{\text{SR}}$ is all corrections of short-range interaction potentials as there were defined to act between the ionic shells.

In case of the single $\text{Nb}^{5+}\text{O}^{2-}$ pair we only considered oxygen-ion displacements along the [100] cubic crystal direction parallel to the molecular pair. In Fig. 2 the corresponding short-range $\text{Nb}^{5+}-\text{O}^{2-}$ potentials are shown with and without polarization correction. The polarization correction has been estimated by considering the additional influence of polarizing basis functions. This method is only applicable, if the basis set without polarizing functions is sufficiently accurate in SCF calculations of correspondingly symmetrical molecules. Our chosen basis set is assumed to fulfill this condition (at least partly in order to estimate polarization effects) because of its considerable variational degree of freedom. We recall that contracted basis functions referring to the rather unstable O 2p electrons have been totally broken down into their constituting primitives. In addition, a diffuse p function has been implemented.

Whereas the simple pair-cluster model worked well in purely ionic crystals (e.g., Refs. 5 and 9), it yields a totally unsatisfactory crystal description of the more covalent KNbO_3 . This result is independent of the inclusion of the polarization term.

In the case of the $(\text{NbO}_6)^{7-}$ quantum cluster we investigated two different sets of calculations. In the first one, breathing-mode distortions of the octahedral cluster in an otherwise unchanged point-ion lattice have been performed in order to derive the required potential. Except at the perfect lattice spacing one has to face the problem of electronic polarization of the oxygen ions which can be understood principally by symmetry arguments.²¹ However, there is no way to obtain appropriate quantitative information concerning this polarization from an analysis of the charge density. Since all cluster multipole mo-

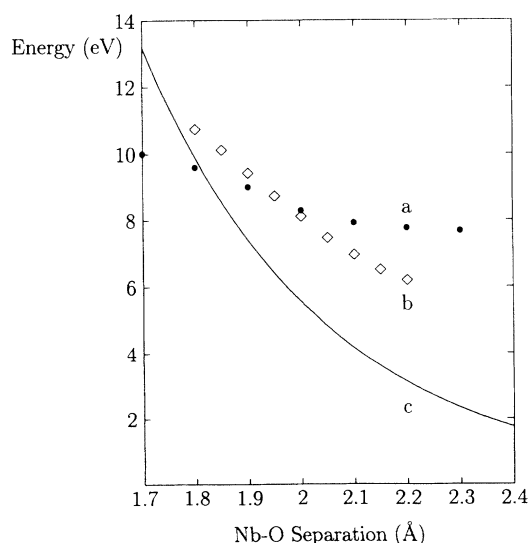


FIG. 2. *Ab initio* potential derived from a simple pair of ions. (a) *Ab initio* potential (●) from a $\text{Nb}^{5+}\text{O}^{2-}$ quantum pair without polarization correction. (b) *Ab initio* potential (◇) from a $\text{Nb}^{5+}\text{O}^{2-}$ quantum pair including polarization correction. (c) Empirical $\text{Nb}^{5+}-\text{O}^{2-}$ potential for comparison.

ments vanish up to hexadecapole moments, the method proposed by Harding and Harker⁸ is not useful in this case. Asymmetrical cluster distortions could be investigated alternatively, however, we defer such calculations to the future. Instead we employed another approach which can be termed hydrostatic pressure simulation. Here, the whole crystal is shrunk or expanded corresponding to a change of the cubic lattice constant. Thus, at each Nb-O separation the system pertains the perfect cubic lattice symmetry. As a result there are essentially no electronic polarization effects and the short-range potential obtained this way does not need any further polarization corrections. We note that calculations without additional polarizing basis functions could be attempted as well, but we found it more attractive in this case to use the hydrostatic pressure simulation, where polarizing functions remained included. The present approach is physically more significant, since it tests by construction the pressure dependence of the NbO_6 crystal fragment, whereas the previous method seems to be more artificial, because polarization terms have been extracted by purely mathematical manipulations. Our procedure of applying hydrostatic pressure is similar to one known in literature as “potential induced breathing” (PIB) method.²² Different from PIB, however, we employed SCF-MO calculations in which covalency effects as occurring in semi-ionic materials are taken into account. Moreover, since at present our potentials are constrained to be used in simple shell model investigations of KNbO_3 based on pairwise central forces we may not expect to describe any deviations from Cauchy’s condition $C_{12}=C_{44}$ (see Table II, Sec. III A). This equality must hold for unstressed cubic crystals if pairwise central forces are specified to act between the ionic components.

Our results concerning the octahedral $(\text{NbO}_6)^{7-}$ cluster are shown in Fig. 3. We emphasize the very satisfactory agreement between the empirical and the *ab initio* hydrostatic potential at relevant ion separations around 2 Å (note that both potential generation methods are essentially different by construction). This outcome indicates that potential parameters which were derived by empirical fitting need not necessarily correspond to physically meaningless numbers but can bear some physical relevance, which supports shell-model simulations based on careful empirical parametrizations. Both $\text{Nb}^{5+}-\text{O}^{2-}$ potentials provide useful descriptions of KNbO_3 crystals (Sec. III). The deviations of the short-range potential which was derived from breathing-mode cluster distortions are caused by the electronic polarization term E_{pol} discussed earlier. Subsequently, we do not consider the latter potential. It could, however, at least be useful within a totally rigid-ion crystal model.

We relate the differences between the NbO pair and the NbO_6 cluster results mainly to covalency effects, which are largely suppressed in the simple pair model. The ionic charges obtained by a Mulliken population analysis remained close to the pure ionic values in the case of the pair model (Nb^{5+} : $q \approx +4.75|e|$, O^{2-} : $q \approx -1.75|e|$), but showed significant deviations, in particular for the Nb ion, in the cluster model (Nb^{5+} : $q \approx +2.84|e|$, O^{2-} : $q \approx -1.64|e|$). One may think of the short-range

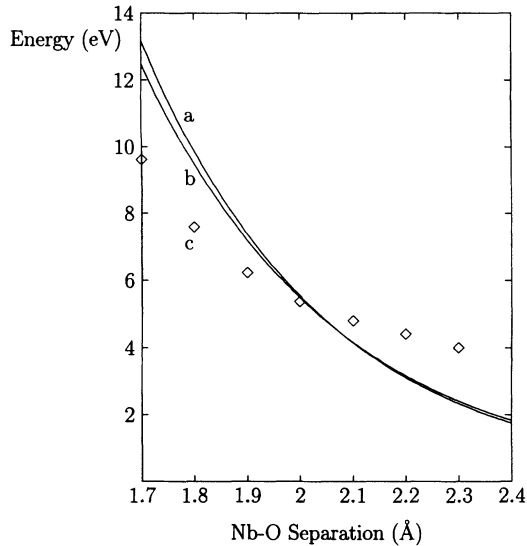


FIG. 3. *Ab initio* potential derived from an embedded NbO_6 quantum cluster. (a) Empirical $\text{Nb}^{5+}-\text{O}^{2-}$ potential for comparison. (b) *Ab initio* hydrostatic potential involving a $(\text{NbO}_6)^{7-}$ quantum cluster. The potential has been calculated from breathing-mode distortions of the whole crystal. This simulates the application of a hydrostatic pressure. The potential does not need polarization corrections. (c) *Ab initio* potential (\diamond) from a $(\text{NbO}_6)^{7-}$ quantum cluster without polarization correction. The potential has been calculated from breathing-mode distortions of the quantum cluster in an otherwise unchanged lattice.

$\text{Nb}^{5+}-\text{O}^{2-}$ interaction being more effectively screened within the octahedral cluster model. Put another way, the various short-range interionic potentials in a semionic material cannot be considered as being independent from each other (which, however, we expect to be sufficiently correct for pure ionic crystals). In KNbO_3 this concerns the $\text{Nb}^{5+}-\text{O}^{2-}$ and the $\text{O}^{2-}-\text{O}^{2-}$ interactions; by means of the NbO_6 cluster a consistent treatment of these potentials should be guaranteed. In contrast the K^+-O^{2-} interaction is far more ionic in nature. Besides the $\text{O}^{2-}-\text{O}^{2-}$ interaction we retained this potential from earlier simulation studies.²³ In Table I all short-range interactions are summarized which were used in our subsequent investigations. Figure 4 shows a graphical display of these short-range potentials. The relative importance of the $\text{Nb}^{5+}-\text{O}^{2-}$ short-range interaction is clearly seen.

TABLE I. Short-range potential parameters as used in subsequent shell-model simulations.

Interaction Type	A/eV	$\rho/\text{\AA}$	$C/\text{eV \AA}^6$
$\text{O}^{2-}-\text{O}^{2-}$	22 746.30	0.149 00	27.88
$\text{Nb}^{5+}-\text{O}^{2-}$ (<i>ab initio</i>)	1 333.44	0.364 04	0.0
(empirical)	1 796.30	0.345 98	0.0
K^+-O^{2-}	1 000.30	0.361 98	0.0

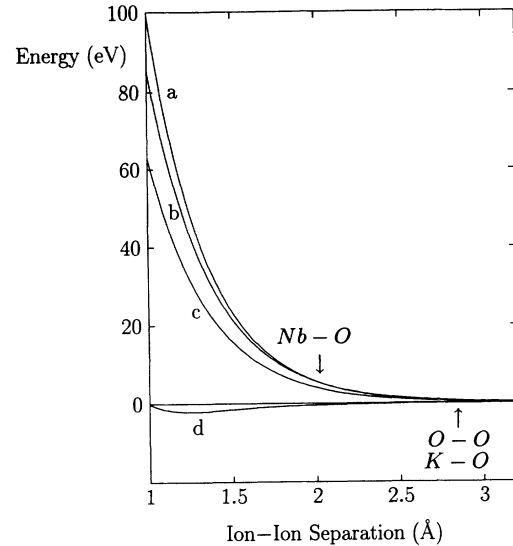


FIG. 4. Short-range potentials relevant for KNbO_3 . Arrows denote equilibrium ion-ion separations. (a) Empirical $\text{Nb}^{5+}-\text{O}^{2-}$ potential. (b) *Ab initio* $\text{Nb}^{5+}-\text{O}^{2-}$ potential from $(\text{NbO}_6)^{7-}$ cluster. Its derivation involved a hydrostatic distortion of the whole crystal (see text). (c) Empirical K^+-O^{2-} short-range potential. (d) Empirical $\text{O}^{2-}-\text{O}^{2-}$ short-range potential.

III. RESULTS OF SHELL-MODEL SIMULATION STUDIES IN KNbO_3 AND KTaO_3

In this section we present some results obtained from shell-model simulations of perfect and defective KNbO_3 using the *ab initio* hydrostatic $\text{Nb}^{5+}-\text{O}^{2-}$ short-range potential. These calculations are compared with corresponding ones employing the empirical interaction. Finally, we discuss possible off-center displacements of Nb^{5+} ions incorporated in a KTaO_3 host crystal on a Ta site. All calculations have been done using the shell-model program code CASCADE.²⁴

A. Perfect lattice simulations

First of all, we note that both the empirical as well as the *ab initio* $\text{Nb}^{5+}-\text{O}^{2-}$ short-range potential generate the cubic phase of KNbO_3 but no ferroelectric phases. Using the *ab initio* potential the lattice constant of KNbO_3 is overestimated by only 0.47% (but 1.67% employing the empirical potential). Description of ferroelectric phases would probably demand us to go beyond the pair-potential and dipole polarizable ion approximation, to include electronic correlation, to perform calculations for a wider range of cluster geometries (differing from the breathing mode), and to investigate suitable supercell calculations in order to catch some of the cooperative phenomena governing ferroelectricity. As we are mainly interested in the calculation of defect energies it is sufficient to employ the present *ab initio* hydrostatic potential, because energetical differences between the various crystallographic phases are very small compared with usual defect energies.

In Table II we compare macroscopic crystal properties

TABLE II. Calculated and experimental macroscopic crystal properties of KNbO_3 .

Property	Calculated		Observed ^{a,b}
	<i>ab initio</i>	empirical	
C_{11} (10^{10}Nm^{-2})	39.788	43.349	25.5
C_{12} (10^{10}Nm^{-2})	14.178	13.114	8.0
C_{44} (10^{10}Nm^{-2})	14.178	13.114	9.0
ϵ_0	4.884	23.789	
ϵ_∞	1.000	1.806	
Lattice constant (\AA)	4.026	4.073	4.007

^aA. C. Nunes, J. D. Axe, and G. Shirane, *Ferroelectrics* **2**, 291 (1971).

^bE. Wiesendanger, *Ferroelectrics* **6**, 263 (1974).

of KNbO_3 calculated using the *ab initio* and the empirical $\text{Nb}^{5+}-\text{O}^{2-}$ potential. Note that at this stage no shell parameters have been defined for Nb^{5+} and O^{2-} ions in combination with the *ab initio* interaction; remember that the hydrostatic procedure does not allow one to derive these parameters (below, however, we shall discuss *ad hoc* introduced ion polarizabilities and their influence on calculated crystal properties).

By inspection of Table II it is observed that the *ab initio* $\text{Nb}^{5+}-\text{O}^{2-}$ potential provides a satisfactory description of structural and elastic properties of cubic KNbO_3 . In fact, these entities are mainly influenced by interionic potentials and not by shell parameters. From this observation we may conclude that our approach is sufficiently accurate in order to derive the required interionic potential. We note that the observed deviations between calculated and experimental elastic properties are much more a consequence of the simplifying restrictions imposed *a priori* upon the potential model, e.g., pair potentials in the central field approximation and dipole polarizable ions. Corresponding deviations have been already observed in case of the cubic and ionically bonded MgO . Many-body corrections turned out to be sufficient in order to correct for the deficiencies immanent in simple shell-model simulations (see Ref. 5, for example).

In addition we report that niobium pentoxide Nb_2O_5 , consisting of distorted and irregularly arranged NbO_6 octahedra, is as well reasonably simulated using the *ab initio* $\text{Nb}^{5+}-\text{O}^{2-}$ potential. The *ab initio* model is considerably less strained with respect to the observed structure than the empirical one. In conclusion it seems that the *ab initio* $\text{Nb}-\text{O}$ interaction (although similar to the empirical potential) is slightly better suited for simulation studies of the oxides discussed so far than the empirical counterpart.

In contrast to structural and elastic properties the dielectric behavior is very sensitive to the choice of shell parameters, as is shown in Table III. In particular the static dielectric constant may be fitted to each arbitrary value by changing the shell parameters appropriately. Figure 5 displays the static dielectric constant as a function of the niobium harmonic spring constant. Of course, a similar plot may be generated if the oxygen harmonic spring constant is varied instead. However, it seems very instructive that appropriately changing the polarizability

TABLE III. Calculated dielectric behavior of KNbO_3 as a function of ionic polarizabilities using the *ab initio* hydrostatic $\text{Nb}-\text{O}$ potential.

Variation of k_{Nb} ($\text{eV}\text{\AA}^{-2}$) ($k_{\text{O}}=103.07\text{ eV}\text{\AA}^{-2}$)	ϵ_0	ϵ_∞
∞	7.703	1.680
2500.0	31.323	1.775
2200.0	100.510	1.790
2120.0	431.690	1.795
2100.0	3937.908	1.796

Variation of k_{O} ($\text{eV}\text{\AA}^{-2}$) ($k_{\text{Nb}}=2500.0\text{ eV}\text{\AA}^{-2}$)	ϵ_0	ϵ_∞
90.0	71.649	1.775
85.0	179.332	1.910
83.0	517.565	2.005
82.0	> 10000	2.021

of niobium ions, which are significantly less polarizable than oxygen ions ($\alpha_{\text{O}}/\alpha_{\text{Nb}} \approx 9$ according to our shell parameters), leads to a sort of ferroelectric instability of the modeled KNbO_3 .

Now, in order to derive a physically reasonable shell parameter set, we suggest the following model, which is certainly empirical at the present stage of our investigations and we need to obtain independent *ab initio* based arguments in favor of this model from further studies. First, we essentially retain the empirical oxygen shell parameters (i.e., $Y_{\text{O}} = -2.811|e|$, $k_{\text{O}} = 103.07\text{ eV}\text{\AA}^{-2}$) from the successful simulation studies of the related material KNb_3O_8 .²⁰ Second, potassium ions are simulated as being unpolarizable because of their pronounced ionic nature. Third, with respect to Nb^{5+} we only consider variations of the harmonic spring constant k_{Nb} , while keeping the shell charge equal to the empirical value (i.e., $Y_{\text{Nb}} = -4.496|e|$). This procedure, although being oversimplified, is sufficient in order to investigate the

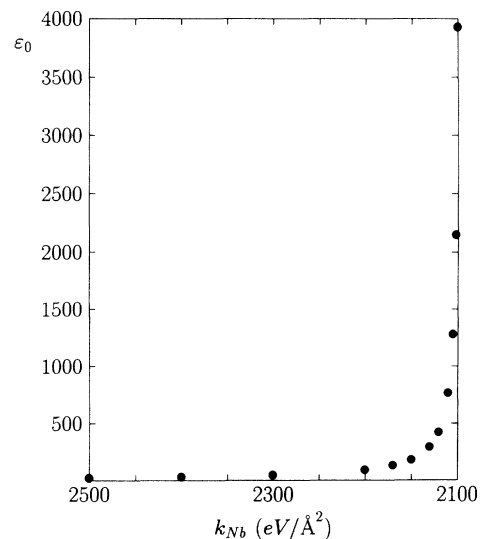


FIG. 5. The static dielectric constant as a function of the niobium core-shell harmonic spring constant.

effects of ionic polarizabilities. Moreover, we choose k_{Nb} close to its instability value.

The qualitative justification of our model concerning ionic polarizabilities is as follows: Since we know that KNbO₃ is unstable against ferroelectric phase transitions, we choose both oxygen and niobium related shell parameters (i.e., core-shell spring constants) to be close to their respective instability region (see Table IV, Fig. 5). The importance of ionic polarizabilities with respect to a ferroelectric behavior has already been stressed by Bilz, Benedek, and Bussmann-Holder.²⁵ However, in contrast to our model these authors ascribe the dominant contributions to the oxygen polarizability. Such an interpretation could be supported by suitable shell-model simulations, in particular the TO-phonon softening has been reproduced this way. On the other hand, Cohen²⁶ pointed out that the oxygen polarizability cannot exclusively be responsible for ferroelectricity to occur. He argues that covalency in terms of hybridizations between O 2*p* and Nb 4*d* orbitals is even more important. This conclusion has been drawn from electronic structure calculations based on the linear augmented plane wave (LAPW) method.²⁷ However, Cohen also claims that shell-model simulations would not be able to shed any light on the physical origin of ferroelectricity as these types of physically simplified calculations involve a set of adjustable parameters which allow to fit ferroelectric properties. We take an intermediate point of view and try to combine both interpretations to some extent: In general the electronic structure of the respective crystals is assumed to represent the basic driving force of ferroelectricity. In particular we anticipate from Cohen that covalency effects between oxygen and niobium (or generally, between oxygen and B cations when referring to ABO₃ perovskites) are essential. Such electronic structure effects, however, may be reasonably well modeled by means of suitable shell-model calculations. It is certainly true that these types of simulations correspond to a simplified view of crystal physics and one has to take care when deriving shell-model parameters in order to avoid an unphysical arbitrariness. It is, for example, helpful to

generate appropriate interionic potentials from *ab initio* calculations (as we have done in this paper) or to start empirical fitting procedures by transferring potential parameters from simpler, well understood systems to the actual crystals under investigation. Moreover, it seems reasonable to compare shell-model parameter sets of different but closely related materials, as KNbO₃ and KTaO₃ in the present context. Whereas KNbO₃ undergoes ferroelectric phase transitions, these are inhibited in KTaO₃. KTaO₃ is often called to be an incipient ferroelectric, describing its property of exhibiting a large static dielectric constant at low temperatures which is not accompanied by a ferroelectric phase transition. Since the obvious difference between both crystals, which have the same lattice structure with almost equal interionic separations, is provided by the different B cations, the differences in ferroelectric behavior should be related to these cations. Indeed, if we compare shell-model simulations of KNbO₃ and KTaO₃ using empirical parameter sets (detailed results of which will be published shortly) we observe that first, the Ta-O short-range interaction is slightly more repulsive than both the *ab initio* and the empirical Nb-O potential and that second, Nb ions are more polarizable than Ta ions but oxygen in KNbO₃ is less polarizable than in KTaO₃. We observe $\alpha_{\text{O}}/\alpha_{\text{Ta}} \approx 70$ inserting the appropriate shell parameters, thus being significantly larger than in KNbO₃. It is noted in this context, that regarding KTaO₃ only the oxygen polarizability is near to its instability value, whereas in case of KNbO₃ this is true for both the oxygen and the niobium polarizability. The reason for these differences might be a more ionic bonding between tantalum and oxygen ions. A less pronounced charge transfer in KTaO₃ crystals would cause the oxygen ions to remain more polarizable than in KNbO₃, whereas Nb ions, in turn, should be more polarizable than Ta ions. Covalent charge transfer from oxygen onto the octahedrally coordinated metal ion stabilizes the oxygen ions, which are then less negative, and destabilizes the metal ion because of its increased electronic charge. This covalency related interpretation of shell-model ionic polarizabilities is supported by our

TABLE IV. Formation energies (eV) of important intrinsic defects in KNbO₃.

Defect	<i>ab initio</i> Nb-O potential				Empirical Nb-O potential				
	$k_{\text{O}} = 103.07 \text{ eV \AA}^{-2}$ $k_{\text{Nb}} \text{ (eV \AA}^{-2}\text{)}$	2100.0	2300.0	2500.0	∞	$k_{\text{Nb}} = 2500.0 \text{ eV \AA}^{-2}$ $k_{\text{O}} \text{ (eV \AA}^{-2}\text{)}$	90.0	83.0	$k_{\text{O}} = 103.07 \text{ eV \AA}^{-2}$ $k_{\text{Nb}} \text{ (eV \AA}^{-2}\text{)}$
V_{Nb}^{I}	119.57	121.90	123.57	133.29	121.44	119.99	134.79		
V_{O}^{I}	19.68	19.83	19.94	20.83	19.74	19.62	21.00		
V_{K}^{I}	3.99	4.03	4.06	4.31	4.02	4.00	4.11		
$\text{Nb}_{\text{K}}^{\text{I}}$	-109.69	-109.32	-109.03	-106.90	-109.51	-109.83	-109.37		
$\text{Nb}_{\text{I}}^{\text{I}}$	-102.43	-101.34	-100.51	-94.19	-101.55	-102.25	-94.93		
K_{I}	3.87	3.95	4.05	4.38	3.95	3.90	5.87		
$\text{O}_{\text{I}}^{\text{I}}$	-7.31	-7.00	-6.78	-5.54	-7.23	-7.60	-5.90		
$\text{Nb}_{\text{Nb}}^{\text{I}}$ (thermal)	44.72	44.82	44.88	45.39	44.75	44.65	45.88		
$\text{Nb}_{\text{Nb}}^{\text{I}}$ (optical)	48.44	48.46	48.47	48.61	48.16	47.96	48.72		
$\text{O}_{\text{O}}^{\text{I}}$ (thermal)	17.42	17.48	17.52	17.85	17.46	17.43	18.08		
$\text{O}_{\text{O}}^{\text{I}}$ (optical)	23.16	23.18	23.19	23.34	23.05	22.95	23.21		

ab initio cluster calculations on NbO₆ and TaO₆, as a Mulliken population analysis pointed to increased covalency in the case of the NbO₆ cluster. The stronger ionicity of the Ta-O bond compared to Nb-O has also been stressed by Thomann.²⁸ In line with his reasoning we feel the degree of ionicity within the oxygen octahedra to be crucial for the occurrence of ferroelectricity. Covalency manifests itself in shell-model simulations in that it influences an ionic and cationic polarizabilities as well as the functional form of the interionic short-range potential between these species. The above discussion suggests that the oxygen polarizability cannot exclusively account for ferroelectricity, since otherwise KTaO₃ would be ferroelectric and not KNbO₃ if we take the degree of oxygen polarizability as a measure. This observation, finally, led us to choose both the oxygen and the niobium polarizability within their respective instability region. The fact that (beyond anion polarizabilities and interionic potentials) the Nb (or generally the B cation) polarizability is of particular importance will be further supported by our defect calculations which are presented in the next section. Here, we only note that the Nb polarizability ultimately allows these ions to move off center from the octahedral cubic lattice site. This behavior which is related to ferroelectricity cannot be modeled by means of oxygen polarizabilities.

B. Defect simulations

In Table IV we report defect-formation energies for the most important intrinsic defects in KNbO₃ using the *ab initio* Nb⁵⁺-O²⁻ potential for various choices of shell parameters. For comparison defect energies calculated on the basis of the empirical model have been listed, too. As point defects destroy the translational symmetry of perfect crystals, the shell-model program CASCADE determines defect energies by means of the two-region strategy⁵ and the Mott-Littleton approximation.²⁹

We observe from Table IV that corresponding defect energies vary by an amount between 5 and 20 % as a function of ionic polarizabilities. As expected, defect energies decrease with increasing ionic polarizability.

Moreover, the application of the *ab initio* Nb⁵⁺-O²⁻ potential leads to smaller defect energies as compared to the empirical model. The defect chemical properties of KNbO₃, however, remain qualitatively unaltered upon these changes. As the defect chemistry will be discussed at some length in a forthcoming publication,³⁰ it suffices in the present context to remark on certain quantitative aspects of defect properties calculated using the *ab initio* and the empirical Nb⁵⁺-O²⁻ potential. In Table V we have summarized the relevant formation energies concerning Frenkel and Schottky disorder, electronlike and holelike polarons and, finally, the electronic gap.

In the case of Frenkel- and Schottky-type disorder we note that all reaction energies decrease in line with single defect energies, if the *ab initio* potential is used with increasing degrees of ionic polarizability. In particular, Nb⁵⁺ Frenkel disorder as well as Nb₂O₅ and NKbO₃ related Schottky-type defects take advantage of these changes. In spite of this all defects remain energetically unfavorable in order to be created with higher concentrations in KNbO₃ crystals.

A shell-model treatment of surplus electron or hole species implies a small polaron model. The stability criterion favoring small polarons against large polarons or bandlike states is given by

$$|\Delta E_B| > \frac{\Delta}{2}, \quad (3.1)$$

where ΔE_B is the small polaron binding energy listed in Table V and Δ is the appropriate bandwidth. The small polaron binding energy is defined as the difference of the optical and the thermal polaron defect energy, where optical means that only ionic shells are allowed to relax and thermal a full relaxation of cores and shells. The right-hand side of Eq. (3.1) represents the gain in delocalization energy in a band model which may be considered to be competitive with small polaron formation. In the case of electrons (Nb_{Nb}⁴⁺) the conduction bandwidth is $\Delta_{CB}=3$ eV,³¹ and in the case of holes (O_O¹⁻) the width of the valence band $\Delta_{VB}=5$ eV.³¹ From this we predict the for-

TABLE V. Calculated defect chemical properties involving intrinsic defects.

Defect type	<i>ab initio</i> Nb-O potential						Empirical Nb-O potential
	$k_O = 103.07 \text{ eV \AA}^{-2}$	$k_{Nb} = 2500.0 \text{ eV \AA}^{-2}$	$k_O = 103.07 \text{ eV \AA}^{-2}$	$k_{Nb} = 2500.0 \text{ eV \AA}^{-2}$	$k_O = 103.07 \text{ eV \AA}^{-2}$	$k_{Nb} = 2500.0 \text{ eV \AA}^{-2}$	$k_O = 103.07 \text{ eV \AA}^{-2}$
	2100.0	2300.0	2500.0	∞	90.0	83.0	1358.58
Frenkel disorder, energy per defect (eV)							
K ⁺	3.93	3.99	4.06	4.34	3.99	3.95	4.99
Nb ⁵⁺	8.57	10.28	11.53	19.55	9.94	8.87	19.93
O ²⁻	6.18	6.41	6.58	7.65	6.26	6.01	7.55
Schottky-type disorder, energy per defect (eV)							
K ₂ O	1.75	1.83	1.89	2.35	1.80	1.74	2.27
Nb ₂ O ₅	2.08	2.85	3.41	6.82	2.66	2.15	7.37
KNbO ₃	1.80	2.36	2.77	5.30	2.22	1.85	5.70
Electron and hole polarons, $\Delta E_B = E_{\text{optical}} - E_{\text{thermal}}$ (eV)							
Nb _{Nb} ⁴⁺	3.72	3.64	3.59	3.22	3.41	3.31	2.84
O _O ¹⁻	5.74	5.70	5.68	5.49	5.58	5.53	5.13
Electronic gap, charge-transfer energy O ²⁻ → Nb ⁵⁺ (eV)							
	2.85	2.99	3.10	3.94	2.91	2.78	4.66

mation of small electron and hole polarons to be favored over bandlike species for all potential models considered so far. This result becomes more pronounced the larger the calculated static dielectric constant is (compare Tables III and V). We note that the static dielectric constant essentially measures the possible degree of lattice relaxation as a consequence of charged defects.

Finally, Table V shows our calculated electron transfer energies from an oxygen ion onto niobium. As oxygen $2p$ states define the valence band and niobium $4d$ states the conduction band, we may interpret the charge-transfer energy to give the electronic band gap. Again we found smaller gap energies when using the *ab initio* potential in combination with niobium polarizabilities in the specified region above the expected "phase transition" (see Fig. 5). Experimentally, the gap energy has been reported to be 3.1 eV,³² which is in good agreement with our calculations.

We conclude our considerations by studying possible off-center displacements of Nb^{5+} ions which are incorporated in a KTaO_3 host crystal on tantalum site. The potential model for KTaO_3 has been derived by empirical fitting to macroscopic properties and crystal structure of this ternary oxide.³⁰ In order to simulate the short-range interaction between the Nb impurity and its nearest oxygen neighbors we used both the empirical and the *ab initio* hydrostatic $\text{Nb}^{5+}-\text{O}^{2-}$ potential combined with niobium polarizabilities as specified in the caption of Fig. 6. Figure 6 shows the Nb incorporation energy (renormalized to the on-center position) as a function of an off-center displacement along one [111] cubic crystal direction. By inspection of the rigid-ion curves we infer that

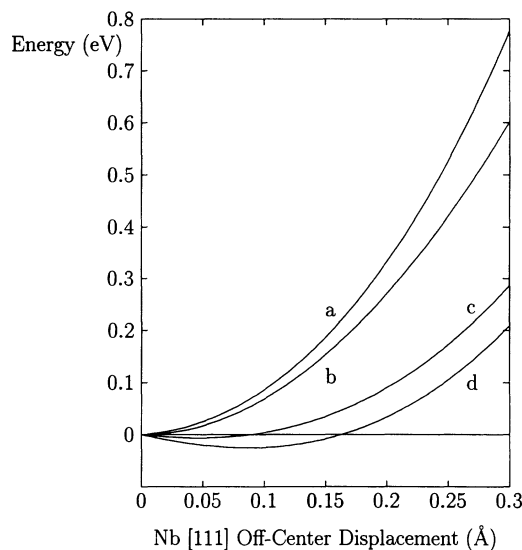


FIG. 6. Off-center displacement (along a [111] cubic crystal direction) of one Nb^{5+} impurity incorporated in KTaO_3 on Ta site. All energies are renormalized with respect to the on-center incorporation energy. (a) Empirical $\text{Nb}^{5+}-\text{O}^{2-}$ potential with $k_{\text{Nb}} = \infty$. (b) *Ab initio* hydrostatic $\text{Nb}^{5+}-\text{O}^{2-}$ potential with $k_{\text{Nb}} = \infty$. (c) Empirical $\text{Nb}^{5+}-\text{O}^{2-}$ potential with $k_{\text{Nb}} = 1358.58 \text{ eV}/\text{Å}^2$. (d) *Ab initio* hydrostatic $\text{Nb}^{5+}-\text{O}^{2-}$ potential with $k_{\text{Nb}} = 2500.0 \text{ eV}/\text{Å}^2$.

the *ab initio* potential is *sui generis* better suited to model ionic off-center displacements which are confirmed experimentally.³³ However, it is the niobium polarizability that (in combination with lattice relaxation) ultimately allows for measurable off-center displacements. This result is valid using both types of potentials. It is readily interpreted by an obvious importance of electronic effects such as covalency. As was argued above, covalency is stronger in the case of niobium ions than in that of tantalum ions. We note that there are no off-center displacements concerning the tantalum. At this stage we again refer the reader to our comments on ferroelectricity in Sec. III A.

The off-center displacement of Nb ions is most pronounced in the case of the *ab initio* interaction. Using $k_{\text{Nb}} = 2500 \text{ eV}/\text{Å}^2$ we find [111] and [110] off-center displacements of about 0.08 Å with an energy gain of 0.017 eV. However, by increasing the Nb polarizability corresponding $k_{\text{Nb}} = 2100 \text{ eV}/\text{Å}^2$ we observe that a niobium displacement along [110] becomes slightly favored against one along [111] (Fig. 7). Since we do not know corresponding experimental results we speculate that a few shortcomings of our model, e.g., the dipole polarizable ion approximation and the neglect of many-body corrections to the interionic potentials, might cause the [110] displacement to be preferred. The energy difference of about 0.04 eV between both crystal directions could be easily delivered by suitable model improvements. Further studies will be useful in order to clarify this point. In spite of these uncertainties, however, we emphasize the following aspects which we consider to represent reliable results of our present simulations:

- Electronic polarizability of Nb ions as well as lattice relaxations around these impurities are necessary for all possible off-center displacements to occur. Indeed, all

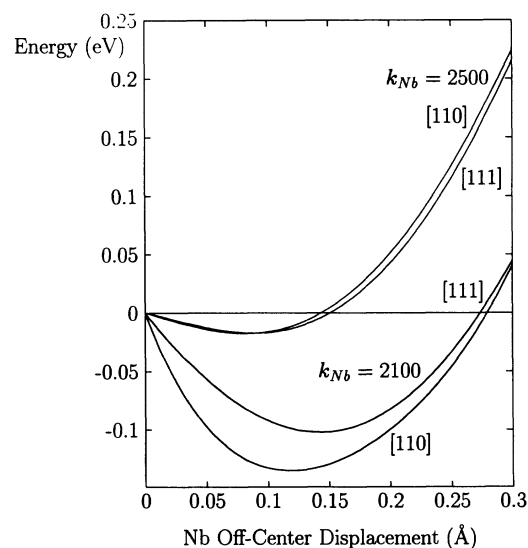


FIG. 7. Niobium off-center displacements along [110] and [111] directions in KTaO_3 . The *ab initio* hydrostatic $\text{Nb}^{5+}-\text{O}^{2-}$ potential has been employed together with two choices for the niobium spring constant. Incorporation energies refer to deviations with respect to the on-center position.

model calculations in which exactly one of these features has been taken into account failed to give a nonvanishing off-center displacement.

● Predicted magnitudes of off-center displacements based on the *ab initio* $\text{Nb}^{5+}-\text{O}^{2-}$ potential are in good agreement with what is known from experiments. The largest displacement ($\approx 0.15 \text{ \AA}$) has been reported from extended x-ray-absorption fine structure measurements.³³

● A pair-potential shell-model treatment is sufficiently sensitive to distinguish Nb^{5+} from Ta^{5+} ions. Different from niobium ions the more ionic tantalum ions do not show any tendency to move off center.

IV. CONCLUSIONS

We have derived an *ab initio* short-range potential simulating the $\text{Nb}^{5+}-\text{O}^{2-}$ interaction in KNbO_3 crystals. Our procedure based on applying hydrostatic pressure to KNbO_3 turned out to be well suited for obtaining the required potential. As this method does not yield shell parameters, we have used empirical reasonings to construct an appropriate set of these parameters. The successful simulations of perfectly cubic and defective KNbO_3 as well as results concerning off-center displacements of Nb impurities incorporated in KTaO_3 strongly

support or methodology.

We emphasize that for a successful potential generation it is necessary to consider a quantum cluster larger than a lone NbO pair in order to appropriately describe covalency contributions which are present in semi-ionic KNbO_3 . This is different from earlier investigations on purely ionic materials.

Finally, in order to achieve further conceptual improvements we propose for future investigations to include asymmetrical cluster distortions and suitable ion size effects on all outer ions immediately surrounding the quantum cluster. In particular the last suggestion would bring the model closer to situations met in real crystals. Moreover, we feel that consideration of additional many-body potential contributions will enable us to model structural phase transitions as observed for KNbO_3 . In particular for this purpose it might be reasonable to combine *ab initio* hydrostatic interionic potentials with a refined shell model.

ACKNOWLEDGMENT

The financial support of this work by the Deutsche Forschungsgemeinschaft (SFB 225) is gratefully acknowledged.

-
- ¹G. V. Lewis and C. R. A. Catlow, *J. Phys. C* **18**, 1149 (1985).
²N. L. Allan and W. C. Mackrodt, *Philos. Mag. A* **58**, 555 (1988).
³H. Donnerberg and C. R. A. Catlow, *J. Phys.: Condens. Matter* **5**, 2947 (1993).
⁴H. Donnerberg, S. M. Tomlinson, C. R. A. Catlow, and O. F. Schirmer, *Phys. Rev. B* **40**, 11 909 (1989); **44**, 4877 (1991).
⁵*Computer Simulation of Solids*, edited by C. R. A. Catlow and W. C. Mackrodt, Lecture Notes in Physics, Vol. 166 (Springer-Verlag, Berlin, 1982).
⁶B. G. Dick and A. W. Overhauser, *Phys. Rev.* **112**, 90 (1958).
⁷R. G. Gordon and Y. S. Kim, *J. Chem. Phys.* **56**, 3122 (1972).
⁸J. H. Harding and A. H. Harker, *Philos. Mag.* **B 51**, 119 (1985).
⁹R. Pandey, X. Yang, J. M. Vail, and J. Zuo, *Solid State Commun.* **81**, 549 (1992).
¹⁰J. Meng, R. Pendey, J. M. Vail, and A. B. Kunz, *Phys. Rev. B* **38**, 10 083 (1988).
¹¹J. Meng, R. Pendey, J. M. Vail, and A. B. Kunz, *J. Phys.: Condens. Matter* **1**, 6049 (1989).
¹²N. C. Pyper, *Philos. Trans. R. Soc. London, Ser. A* **320**, 107 (1986).
¹³W. C. Mackrodt, R. F. Stewart, J. C. Campbell, and I. M. Hillier, *J. Phys. (Paris)* **67**, 64 (1980).
¹⁴P. Saul, C. R. A. Catlow, and J. Kendrick, *Philos. Mag. B* **43**, 597 (1981).
¹⁵C. R. A. Catlow and M. R. Hayns, *J. Phys. C* **5**, L237 (1972).
¹⁶*Gaussian Basis Sets for Molecular Calculations*, edited by S. Huzinaga, J. Andzelm, M. Klobukowski, E. Radzio-Andzelm, Y. Sakai, and H. Tatewaki (Elsevier, Amsterdam, 1984).
¹⁷T. H. Dunning, Jr. and P. J. Hay, in *Methods of Electronic Structure Theory*, edited by H. F. Schaefer III (Plenum, New York, 1977).
¹⁸S. F. Boys and F. Bernardi, *Mol. Phys.* **19**, 553 (1970).
¹⁹R. W. Grimes, C. R. A. Catlow, and A. M. Stoneham, *J. Phys.: Condens. Matter* **1**, 7367 (1989).
²⁰C. R. A. Catlow, C. M. Freeman, M. S. Islam, R. A. Jackson, M. Leslie, and S. M. Tomlinson, *Philos. Mag. A* **58**, 123 (1988).
²¹We note that even at perfect lattice spacings there is a certain asymmetry resulting from embedding the quantum cluster only within a field of point charges representing the outer crystal. However, by cluster calculations with and without polarizing *d*-basis functions we are sure that at the perfect lattice spacing there is only a small polarization induced contribution to the short-range interaction energy ($\leq 0.1 \text{ eV}$) which may safely be neglected to first order. This becomes considerably different the more the niobium-oxygen separation deviates from the perfect lattice spacing.
²²M. J. Mehl, R. J. Hemley, and L. L. Boyer, *Phys. Rev. B* **33**, 8685 (1986).
²³R. A. Jackson and C. R. A. Catlow, *Mol. Sim.* **1**, 207 (1988).
²⁴M. Leslie, *Solid State Ionics* **8**, 243 (1983).
²⁵H. Bilz, G. Benedek, and A. Bussmann-Holder, *Phys. Rev. B* **35**, 4840 (1987).
²⁶R. E. Cohen, *Nature (London)* **362**, 213 (1993).
²⁷R. E. Cohen, *Nature (London)* **358**, 136 (1992).
²⁸H. Thomann, *Ferroelectric* **73**, 183 (1987).
²⁹N. F. Mott and M. J. Littleton, *Trans. Faraday Soc.* **34**, 485 (1938).
³⁰M. Exner, H. Donnerberg, O. F. Schirmer, and C. R. A. Catlow (unpublished).
³¹P. Pertosa and F. M. Michel-Calendini, *Phys. Rev.* **17**, 2011 (1978).
³²E. Wiesendanger, *Ferroelectrics* **6**, 263 (1974).
³³O. Hanske-Petitpierre, Y. Yacoby, J. Mustre de Leon, E. A. Stern, and J. J. Rehr, *Phys. Rev.* **44**, 6700 (1991).

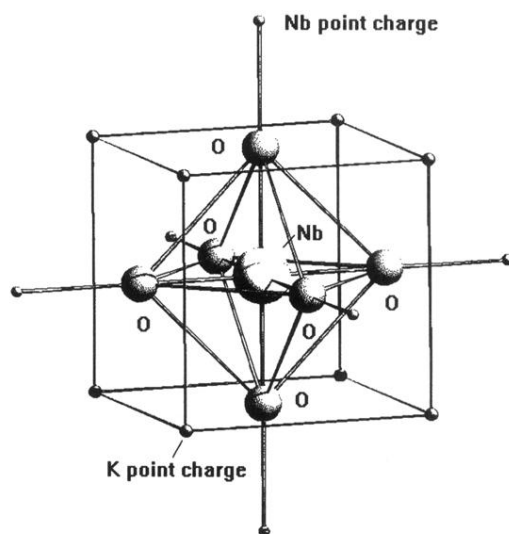


FIG. 1. $(\text{NbO}_6)^{7-}$ quantum cluster with its nearest potassium and niobium (point charge) neighbors. Spheres do not correspond to known ion radii.